January 2007

Structure and magnetic properties of Mn-doped ZnO thin films

Jun Zhang
University of Nebraska - Lincoln

Xingzhong Li
University of Nebraska - Lincoln, xli2@unl.edu

J. Shi
University of Nebraska - Lincoln

Yongfeng Lu
University of Nebraska - Lincoln, ylu2@unl.edu

David J. Sellmyer
University of Nebraska-Lincoln, dsellmyer@unl.edu

Published in *Journal of Physics: Condensed Matter* **19** (2007), 036210 (8 pp) doi:10.1088/0953-8984/19/3/036210 Online at http://stacks.iop.org/JPhysCM/19/036210

Submitted November 2, 2006; published January 5, 2007

Structure and magnetic properties of Mn-doped ZnO thin films

Jun Zhang[1,2], X. Z. Li[2], J Shi[2,3], Y. F. Lu[2,3], and D. J. Sellmyer[1,2]

[1] *Department of Physics and Astronomy, University of Nebraska, Lincoln, NE 68588, USA*

[2] *Nebraska Center for Materials and Nanoscience, University of Nebraska, Lincoln, NE 68588, USA*

[3] *Department of Electrical Engineering, University of Nebraska, Lincoln, NE 68588, USA*

Abstract

We report the structure and magnetic properties of $Zn_{1-x}Mn_xO$ thin films grown on Si(001) substrates by pulsed laser deposition. Structure and phase evolution with Mn doping has been studied using x-ray diffraction, electron diffraction, and high-resolution electron microscopy. The undoped and 1% Mn-doped ZnO films are completely (001) oriented, and further Mn doping deteriorates the (001) orientation. For Mn concentrations below 3%, only the hexagonal ZnO phase exists in the films without secondary phases. As the Mn concentration reaches 5%, secondary phase Mn_2O_3 was found aggregating at grain boundaries. All the Mn-doped films show ferromagnetic properties at room temperature, and the magnetic moment decreases as the Mn concentration increases. Our results suggest that the ferromagnetism observed in $Zn_{1-x}Mn_xO$ thin films is intrinsic rather than associated with secondary phases.

The prediction of high-temperature ferromagnetism (FM) in ZnO-based diluted magnetic semiconductors has stimulated considerable research [1–3]. The Mn–Zn–O system has attracted much attention because of the controversial magnetic properties reported, but their basic origins remain unclear. Both the existence and absence of FM have been reported in Mn-doped ZnO thin films. Spin-glass behavior [4], paramagnetism [5], FM with a T_C of 45 K [6], and room-temperature FM [7] have been observed. This suggests a strong dependence of magnetic properties on the sample-preparation conditions [8]. The recently observed FM in Mn–Zn–O bulk materials synthesized at a low temperature of 500 °C has been argued to arise from the presence of modified manganese oxides, instead of intrinsically from ZnO with Mn substituting for Zn [9, 10]. Kundaliya *et al* [9] proposed that the FM originates from an oxygen–vacancy-stabilized metastable phase, probably in the form of $Mn_{2-x}Zn_xO_{3-\delta}$. Recently, Garcia *et al* [10] associated the FM with a coexistence of Mn^{3+} and Mn^{4+} in manganese oxides via a double-exchange mechanism. In both of these cases, manganese oxides with diffused Zn are considered to be responsible for the FM.

The solubility of Mn in the low-temperature synthesized bulk ZnO is very low, and manganese oxides exist with as little as only 1% Mn doping [8].

It is believed that Mn has higher solubility in ZnO thin films grown by pulsed laser deposition (PLD), which is a non-equilibrium process [11]. Fabrication of Mn-doped ZnO thin films without manganese oxides can facilitate the investigation and understanding of the magnetic properties of this material. In this paper, we report a systematic study of the structure and magnetic properties of Mn-doped ZnO thin films grown by PLD, with special attention given to examining the possible existence of manganese oxides or other impurity phases. We found that for Mn concentrations below 3%, no manganese oxides exist in the Mn-doped ZnO thin films, while as Mn concentration reaches 5%, Mn_2O_3 was found aggregating at grain boundaries. But FM is observed at low Mn concentrations, without the presence of any impurity phase.

Mn-doped ZnO ($Zn_{1-x}Mn_xO$, x = 0–0.05) thin films were grown on Si(001) substrates by PLD. $Zn_{1-x}Mn_xO$ ceramic targets were prepared by standard solid-state reaction. The base pressure of the PLD chamber was 2×10^{-7} Torr. During film growth the oxygen pressure in the chamber was kept at 5×10^{-4} Torr and the substrate temperature was 500 °C. The film thickness varies from 200 to 600 nm. Energy dispersive x-ray spectroscopy (EDS) was used to measure the Mn concentrations. The film structure was characterized using x-ray diffraction, electron diffraction, and high-resolution electron microscopy. Magnetic measurements were made in a superconducting quantum interference device (SQUID) magnetometer (Quantum Design, MPMS-XL).

The film structure was first studied by x-ray diffraction using a Rigaku diffractometer (D/Max-B, Cu Kα, λ = 0.154 nm). Figure 1 shows the x-ray diffraction patterns of $Zn_{1-x}Mn_xO$ thin films with Mn concentration varying from 0 to 5%. The undoped and 1% Mn-doped ZnO films show good (001) orientation, with only (002) and (004) diffraction peaks from the hexagonal ZnO phase. However, as Mn concentration increases up to 3%, the (001) orientation deteriorates. Besides the peaks from the Si substrate, there are strong (002) and (004) peaks and very weak (100) and (103) peaks, all of which belong to the ZnO hexagonal phase, indicating preferred (001) orientation and a small amount of randomly distributed grains. As Mn concentration increases, the ZnO (002) and (004) peaks shift slightly to lower angles. As shown in figure 2, the lattice parameter c derived from the (002) diffraction lines increases as Mn content increases, suggesting that Mn substitutes for Zn in ZnO lattice, at least in the (001) oriented grains. No manganese oxides have been detected according to x-ray diffraction results.

The evolution of the structure properties of the $Zn_{1-x}Mn_xO$ films with increased Mn concentration was further studied using transmission electron microscopy (Jeol JEM2010, 200 kV). Shown in figure 3 are the plane-view high-resolution electron microscopy (HREM) images of $Zn_{1-x}Mn_xO$ thin films with an incident beam parallel to the normal of the film. The HREM image of the film with x = 0.01 (figure 3(a)) shows grains with very clean and sharp grain boundaries, and no secondary phase aggregations are found at grain boundaries. Adjacent grains directly meet each other without separations. The lattice image is clearly visible throughout the whole grains. Within the grains, although there are areas with significant contrast, the array of the spots is continuous across the dark and light areas, suggesting that these areas have the same ZnO hexagonal phase and excluding the possibility that the contrast is due to the existence of different phases. The contrast probably comes from crystal imperfections, such as dislocations or stacking faults. In the centre of the dark areas there are interruptions in the array of spots, indicating the existence of defects.

As the Mn concentration reaches 0.05, however, the HREM image shown in figure 3(b) reveals different features. Grains are separated by aggregations clearly observed at

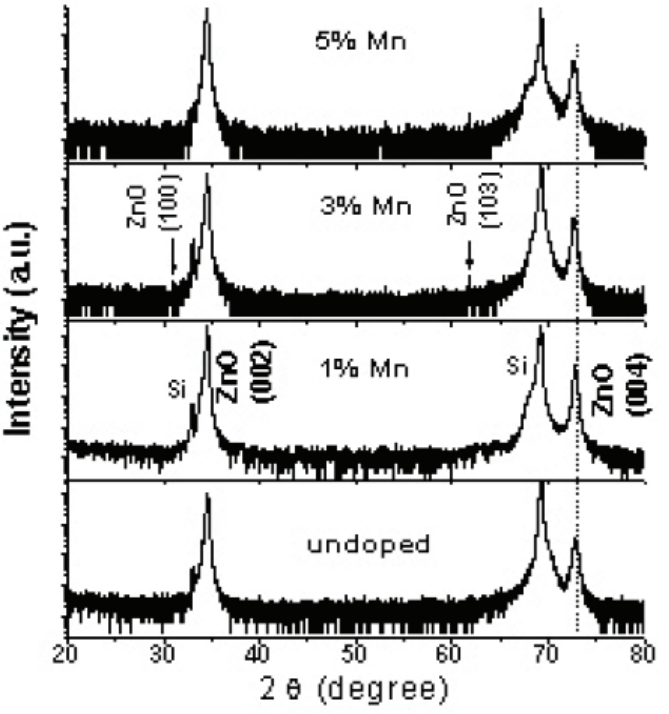

Figure 1. X-ray diffraction pattern of $Zn_{1-x}Mn_xO$ thin films(x = 0, 0.01, 0.03, and 0.05). The intensity axis is plotted on a log scale. The dashed line is plotted to show the shift of the ZnO (004) peak.

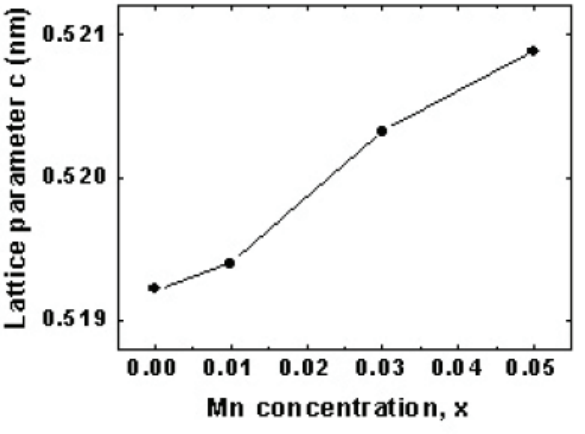

Figure 2. Mn concentration dependence of the lattice parameter c of $Zn_{1-x}Mn_xO$ thin films derived from the (002) spacing.

grain boundaries of 3–5 nm in width. Within the grain boundaries, the lattice image reveals a distinct spot arrangement compared to that in the adjacent grains, indicating that a different structure or phase exists at the grain boundaries.

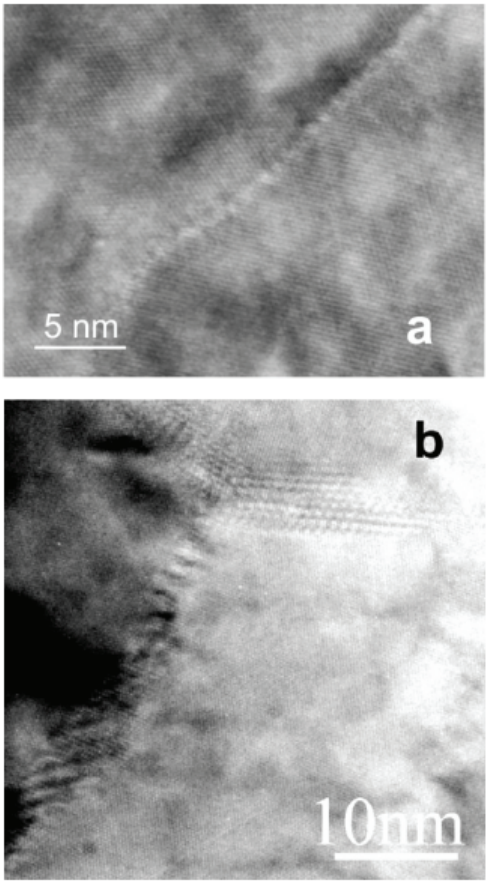

Figure 3. High-resolution electron microscopy images of $Zn_{1-x}Mn_xO$ thin films: (a) x = 0.01; (b) x = 0.05.

Changes in the film structure and phase composition are also revealed by comparing the electron diffraction patterns of the films. Figure 4 shows the polycrystalline electron diffraction patterns of $Zn_{1-x}Mn_xO$ thin films. Figure 4(a) compares the films with x = 0.01 (left) and x = 0.03 (right). Compared with the left pattern, more diffraction rings are observed in the right pattern. All the diffraction rings on the left side from the film with x = 0.01 are indexed consistently with the [001] zone axis of the hexagonal wurtzite ZnO structure, and all the additional diffraction rings appearing in the right pattern from the film doped with x = 0.03 are indexed with wurtzite ZnO structure with random orientation. No evidence was found that manganese oxides or other secondary phases exist in the $Zn_{1-x}Mn_xO$ thin films for x below 0.03. However, as the Mn concentration reaches 5%, as shown in figure 4(b), an extra diffraction ring located within the (100) ring of ZnO was observed. Since (100) is the innermost diffraction ring for ZnO hexagonal structure, this extra diffraction ring is not from hexagonal ZnO, but must be from a secondary phase. Comparing the experimental pattern and simulated results, we conclude that the extra diffraction ring is Mn_2O_3 (211). Although both the x-ray diffraction and electron diffraction results indicate deterioration of the (001) orientation of ZnO thin films with Mn doping, the existence of a Mn_2O_3 secondary phase in 5% Mn-doped ZnO is only revealed by electron diffraction, suggesting that electron diffraction is more powerful than x-ray dif-

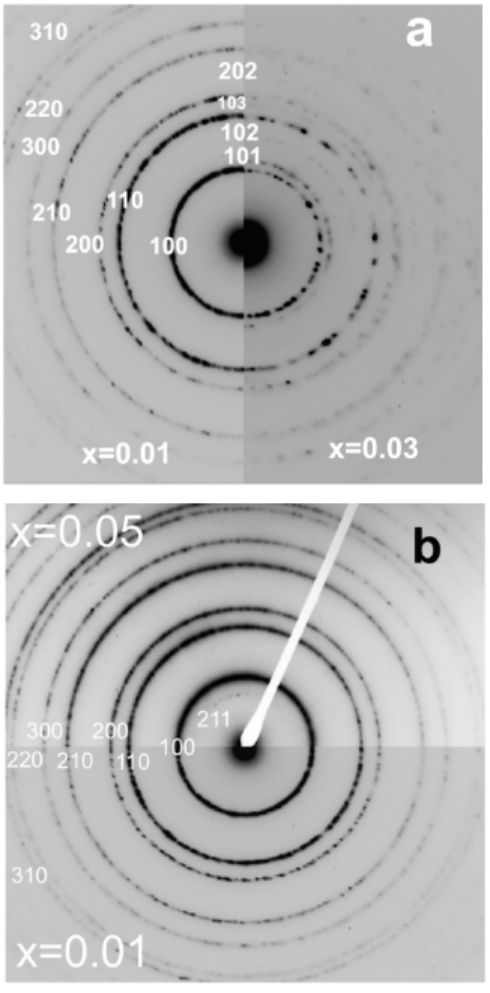

Figure 4. Electron diffraction patterns of $Zn_{1-x}Mn_xO$ thin films. (a) Comparison of x = 0.01 (left) and x = 0.03 (right). For x = 0.01, the diffraction rings are indexed to be (100) to (310) from the centre to the outside; for x = 0.03, only the extra diffraction rings that do not appear at the left-hand side are indexed. (b) Comparison of x = 0.01 (bottom) and x = 0.05 (top). For x = 0.05, the innermost diffraction ring is indexed as Mn_2O_3 (211).

fraction in studying the structure of slightly doped ZnO thin films. The appearance of the Mn_2O_3 secondary phase in the 5% Mn-doped ZnO thin film is consistent with the HREM result shown in figure 3, and it is reasonable to believe that Mn_2O_3 phase aggregates at the grain boundaries.

Magnetization of the $Zn_{1-x}Mn_xO$ thin films was measured at room temperature as a function of the applied magnetic field, as shown in figure 5. The films measured are 200 nm thick. The magnetic field was applied parallel to the film surface, and the diamagnetic contribution from the Si substrate was subtracted. Shown in the bottom inset of figure 5 are the magnetization curves at the low-field range. The magnetization curves show hysteresis, with remanences and the coercivities very similar to those reported for ZnO thin films [12] and nanorods [13] implanted with Mn, suggesting the existence of ferromag-

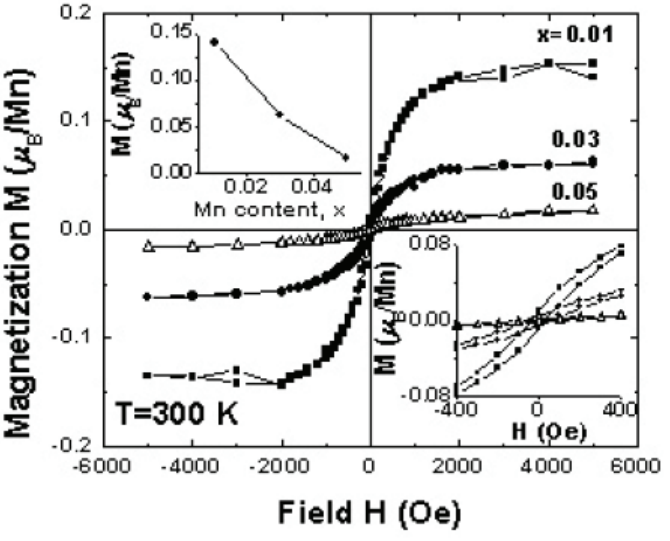

Figure 5. Field dependence of magnetization curves of $Zn_{1-x}Mn_xO$ thin films (x = 0.01, 0.03, and 0.05) at 300 K. Top inset: Mn concentration dependence of the saturation magnetic moment of $Zn_{1-x}Mn_xO$ thin films at 300 K. Bottom inset: enlarged part of the magnetization curves at a low field range.

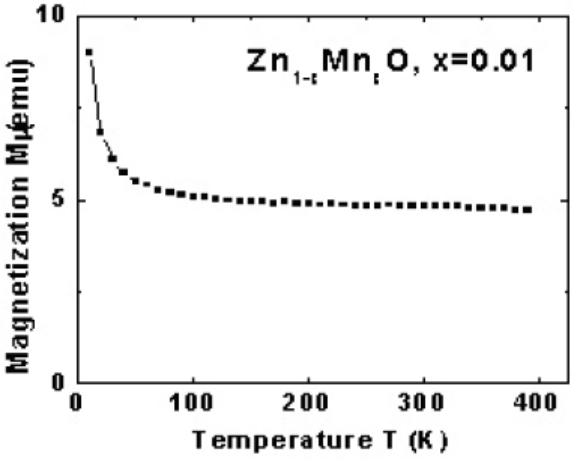

Figure 6. Temperature dependence of magnetization curve of a $Zn_{1-x}Mn_xO$ (x = 0.01) thin film measured at 500 Oe.

netic ordering at room temperature. The top inset of figure 5 shows the Mn concentration dependence of the magnetic moment at 5000 Oe. The moment gradually decreases as the Mn concentration increases. The highest moment observed is about 0.15 μ_B/Mn in the film doped with 1% Mn.

Figure 6 shows the temperature dependence of magnetization measured at 500 Oe for a $Zn_{1-x}Mn_xO$ thin film with x = 0.01. At low temperatures the curve exhibits paramagnetic behavior, with magnetization decreasing quickly as temperature increases. Above 100 K, the magnetization becomes much less sensitive to temperature, and is sustained up to the highest temperature measured (400 K). This temperature dependence of magne-

tization suggests that there is coexistence of a paramagnetic component that is prominent at low temperatures and a ferromagnetic component with a T_C higher than 400 K. By taking into account a combination of a paramagnetic component and a ferromagnetic component, and fitting the paramagnetic component with

$$\chi = \frac{M}{H} = \frac{N\mu_{\text{eff}}^2}{3k_B T},$$

the effective magnetic moment is calculated to be $\mu_{\text{eff}} = 4.75\ \mu_B$/Mn. Assuming that Mn exists as Mn^{2+} and considering that the maximum spin-only moment of Mn^{2+} is 5.92 μ_B/Mn^{2+}, it is estimated that about 64% Mn^{2+} are in a paramagnetic state, for example, being isolated from each other. The low magnetic moment as shown in figure 5 also suggests that only a small fraction of Mn^{2+} participates in the ferromagnetic ordering.

It has been shown that in bulk Zn–Mn–O materials sintered at a low temperature of 500 °C, manganese oxides exist with as little as only 1% Mn doping [8]. But the results reported here show that $Zn_{1-x}Mn_xO$ thin films without secondary phases can be prepared at the same temperature by pulsed laser deposition, which is a non-equilibrium process and may favor the incorporation of Mn into ZnO [11]. Our results also suggest that room-temperature ferromagnetism can be realized in $Zn_{1-x}Mn_xO$ thin films without involving magnetic impurity phases. The mechanism for intrinsic ferromagnetism in $Zn_{1-x}Mn_xO$ still remains unclear. Carrier-mediated ferromagnetism was initially proposed, and it is believed that p-type conductivity favor s this mechanism [1, 2]. An alternative mechanism is the "F-center" model, in which the oxygen vacancy plays an important role [14, 15]. In summary, we have systemically studied the structure and magnetic properties of $Zn_{1-x}Mn_xO$ thin films grown by pulsed laser deposition. Mn doping results in variations in the lattice parameter *c* and deterioration of the (001) orientation of the films. No manganese oxides or other secondary phases are observed in the films with Mn concentrations below 0.03, but the Mn_2O_3 phase appears as the Mn concentration reaches 0.05. Ferromagnetism is observed at room temperature in the $Zn_{1-x}Mn_xO$ thin films and does not appear to be related to manganese oxides or other impurity phases, at least for Mn concentrations below 0.03.

Acknowledgments

This research is supported by the U.S. National Science Foundation Materials Research Science and Engineering Center (NSF-MRSEC), the W. M. Keck Foundation, Nebraska Research Initiative and Nebraska Center for Materials and Nanoscience.

References

[1] Dietl T, Ohno H, Matsukura F, Cibert J, and Ferrand D 2000 *Science* **287** 1019

[2] Sato K and Katayama-Yoshida H 2000 *Japan. J. Appl. Phys.* 2 **39** L555

[3] Pearton S J, Heo W H, Ivill M, Norton D P, and Steiner T 2004 *Semicond. Sci. Technol.* **19** R59

[4] Fukumura T, Jin Z, Kawasaki M, Shono T, Hasegawa T, Koshihara S, and Koinuma H 2001 *Appl. Phys. Lett.* **78** 958

[5] Tiwari A, Jin C, Kvit A, Kumar D, Muth J F, and Narayan J 2002 *Solid State Commun.* **121** 371

[6] Jung S W, An S J, Yi G, Jung C U, Lee S, and Cho S 2002 *Appl. Phys. Lett.* **80** 4561

[7] Sharma P, Gupta A, Rao K V, Owens F J, Sharma R, Ahuja R, Guillen J M O, Johansson B, and Gehring G A 2003 *Nat. Mater.* **2** 673

[8] Zhang J, Skomski R, and Sellmyer D J 2005 *J. Appl. Phys.* **97** 10D303

[9] Kundaliya D, Ogale S, Lofland S, Dhar S, Metting C, Shinde S, Ma Z, Varughese B, Ramanujachary K, Salamanca-Riba L, and Venkatesan T 2004 *Nat. Mater.* **3** 709

[10] García M A, Ruiz-González M L, Quesada A, Costa-Krämer J L, Fernández J F, Khatib S J, Wennberg A, Caballero A C, Martín-González M S, Villegas M, Briones F, González-Calbet J M, and Hernando A 2005 *Phys. Rev. Lett.* **94** 217206

[11] Fukumura T, Jin Z, Ohtomo A, Koinuma H, and Kawasaki M 1999 *Appl. Phys. Lett.* **75** 3366

[12] Heo Y W, Ivill M P, Ip K, Norton D P, Pearton S J, Kelly J G, Rairigh R, Hebard A F, and Steiner T 2004 *Appl. Phys. Lett.* **84** 2292

[13] Ip K, Frazier M, Heo Y W, Norton D P, Abernathy C R, Pearton S J, Kelly J, Rairigh R, Hebard A F, Zavada J M, and Wilson R G 2003 *J. Vac. Sci. Technol.* B **21** 1476

[14] Venkatesan M, Fitzgerald C B, Lunney J G, and Coey J M D 2004 *Phys. Rev. Lett.* **93** 177206

[15] Coey J M D, Venkatesan M, and Fitzgerald C B 2005 *Nat. Mater.* **4** 173